

A HYBRID IMPLICIT-EXPLICIT SPECTRAL FDTD SCHEME FOR OBLIQUE INCIDENCE PROBLEMS ON PERIODIC STRUCTURES

Y.-F. Mao^{1, 2}, B. Chen^{1, *}, H.-Q. Liu¹, J.-L. Xia², and J.-Z. Tang²

¹National Key Laboratory on Electromagnetic Environment and Electro-Optical Engineering, PLA University of Science and Technology, Nanjing, Jiangsu 210007, China

²China Satellite Maritime Tracking and Control Department, Jiangyin, Jiangsu 214400, China

Abstract—This paper combines a hybrid implicit-explicit (HIE) method with spectral finite-difference time-domain (SFDTD) method for solving periodic structures at oblique incidence, resulting in a HIE-SFDTD method. The new method has the advantages of both HIE-FDTD and SFDTD methods, not only making the stability condition weaker, but also solving the oblique incident wave on periodic structures. Because the stability condition is determined only by two space discretizations in this method, it is extremely useful for periodic problems with very fine structures in one direction. The method replaces the conventional single-angle incident wave with a constant transverse wave-number (CTW) wave, so the fields have no delay in the transverse plane, as a result, the periodic boundary condition (PBC) can be implemented easily for both normal and oblique incident waves. Compared with the ADI-SFDTD method it only needs to solve two untridiagonal matrices when the PBC is applied to, other four equations can be updated directly, while four untridiagonal matrices, two tridiagonal matrices, and six explicit equations should be solved in the ADI-SFDTD method. Numerical examples are presented to demonstrate the efficiency and accuracy of the proposed algorithm. Results show the new algorithm has better accuracy and higher efficiency than that of the ADI-SFDTD method, especially for large time step sizes. The CPU running time for this method can be reduced to about 45% of the ADI-SFDTD method.

Received 23 March 2012, Accepted 15 May 2012, Scheduled 27 May 2012

* Corresponding author: Bin Chen (chenbin1957@hotmail.com).

1. INTRODUCTION

Periodic structures have been widely used in electromagnetic applications, such as filters, antenna arrays [1–3], frequency selective surface (FSS) [4], etc. A number of numerical methods have been developed for the simulation of periodic structures in both frequency and time domains [5, 6]. The finite-difference time-domain (FDTD) method is frequently used to analyze periodic structures for it is a transient technique and efficient for wideband applications [7–15]. However, FDTD method has two limitations to simulate incident wave on periodic structures. Firstly, it is an explicit time-marching technique that is subject to the Courant-Friedrich-Levy (CFL) stability condition [16]. To overcome the restriction of the CFL stability condition, an alternating-direction-implicit (ADI) FDTD solution for periodic structures is proposed [17–19], as well as locally-one-dimensional (LOD) FDTD [20–22]. Secondly, the implementation of the periodic boundary condition (PBC) in the time domain is straightforward for the normal incident wave and becomes complicated for the oblique incident because of the time delay in the transverse plane [16]. To deal with this problem, several methods have been introduced, such as Sine-Cosine method [23] and split-field method [24–26]. Recently, another new formulation, named spectral FDTD (SFDTD) was proposed to deal with the problem [27, 28], because the constant wave-number (CTW) wave is used, there is no delay in the transverse plane and the PBC can be implemented directly in the time domain. This scheme has been combined with ADI technique, namely, ADI-SFDTD [19], which eliminates the restriction of the CFL stability condition, also can solve oblique incident wave on periodic structures.

Although the time step in ADI-SFDTD simulations is no longer bounded by the CFL stability condition, the method exhibits dispersion error associated with different time step sizes, which limits the accuracy of the ADI-SFDTD method. Meanwhile, in the ADI-SFDTD method, four untridiagonal matrices, two tridiagonal matrices, and six explicit equations should be solved in one update cycle, which makes it computationally inefficient. To overcome the drawbacks of the ADI-FDTD, recently, a hybrid implicit-explicit (HIE) FDTD method was submitted [29, 30], the computation complexity of the HIE-FDTD method is the same as that of the conventional FDTD method, while the CFL condition restraint is weaker than that of the conventional FDTD method and consequently, less CPU time is required. This advantage can be more obvious when fine structures are involved.

In this paper, the HIE technique is applied to SFDTD method, resulting in a HIE-SFDTD method, which can solve periodic structures

with oblique incident efficiently. The time step in this method is only determined by two space discretizations [30]. To eliminate the time delay in transverse plane, the CTW wave [27] is applied, as a result, the FDTD code needs to be changed from real variables to complex variables, which is different from conventional HIE-FDTD method. Compared with the ADI-SFDTD method it only needs to solve two untridiagonal linear systems when the PBC is applied to, other four equations can be updated directly. The new algorithm has better accuracy and efficiency than the ADI-SFDTD method. Numerical examples are conducted to verify the accuracy and the efficiency of this implementation.

2. IMPLEMENTATION OF THE CTW INCIDENT WAVE

The incident wave is considered as a constant transverse wave-number wave in our discussion, the field components can be seen in Fig. 1.

Because of the CTW wave, the field components are in complex forms, which is not the same as they are in the conventional method. In the time domain, the incident wave can be represented as [27]

$$\begin{aligned}
 E_t^{\text{CTW}} &= \exp(\tilde{j}k_x x) \exp(\tilde{j}k_y y) \xi^{-1} [\exp(\tilde{j}k_z(z-z_0)) \exp(-k_0^2/\sigma^2)] \\
 H_t^{\text{CTW}} &= \exp(\tilde{j}k_x x) \exp(\tilde{j}k_y y) \xi^{-1} [\exp(\tilde{j}k_z(z-z_0)) Y_{TE} \exp(-k_0^2/\sigma^2)] \quad (1) \\
 Y_{TE} &= k_z/\eta_0 k_0
 \end{aligned}$$

where k_x, k_y represent transverse wave-numbers, which are assumed to be constant numbers (independent of frequency). k_z is normal wave-number, $k_0 = 2\pi f/c$, and $\tilde{j} = \sqrt{-1}$. η_0 is the impedance of free space.

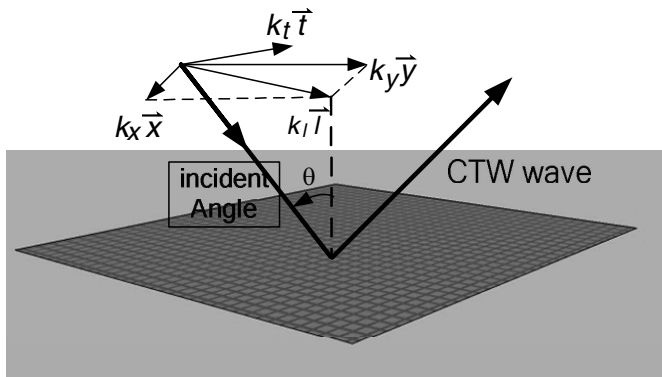


Figure 1. Periodic geometry with CTW incident wave.

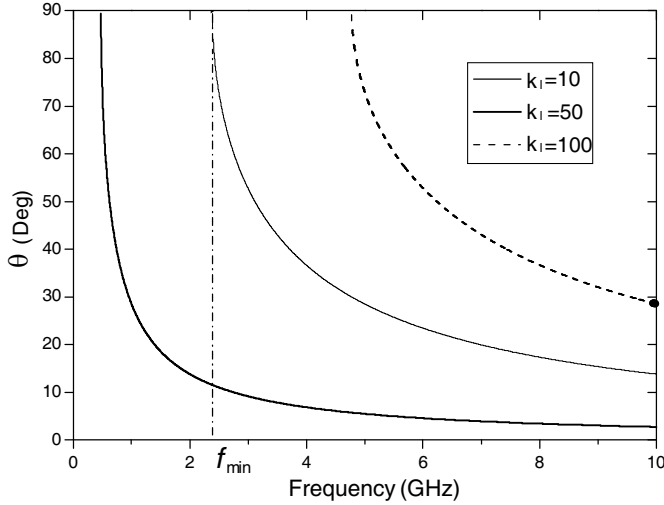


Figure 2. Relation between frequency and incident angle.

The term $\exp(-k_0^2/\sigma^2)$ corresponds to a Gaussian pulse used to limit the bandwidth of incident wave. ξ^{-1} represents the inverse Fourier transform. From Fig. 1 we can see that $\sin(\theta) = k_l/k_0$, if k_x, k_y are constant numbers, that means k_l is constant, so we can conclude that in the CTW wave different frequencies correspond to different incident angles. Fig. 2 shows the relation between the frequency and the incident angle ($k_l = 10, 50, 100$). It can be seen that higher frequencies correspond to smaller angles, when $\theta = 90^\circ$ the minimum frequency is achieved.

3. THEORY AND ALGORITHM IMPLEMENTATION

3.1. Formulation for Hybrid Implicit-Explicit Spectral FDTD

For periodic problems, instead of analyzing the entire structures, only a single-unit cell needs to be considered by incorporating the periodic boundary condition. The computational volume is shown in Fig. 3. In the x - and y -directions, periodic boundary conditions are combined. In the z -direction perfectly matched layers (PML) are used to truncate the simulating region. The total/scattered field (TF/SF) surface is used to add the CTW wave to the computational volume.

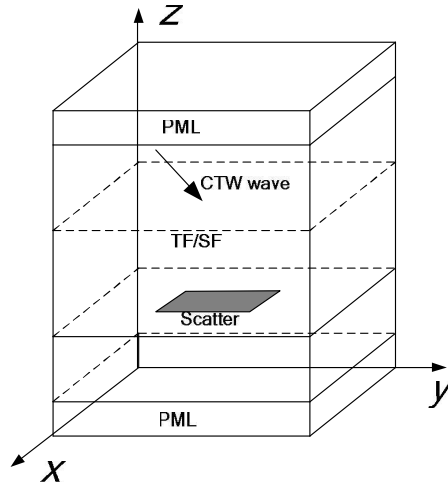


Figure 3. The FDTD computational volume.

The formulations of Maxwell’s curl equations are

$$\nabla \times \vec{H} = \varepsilon \frac{\partial \vec{E}}{\partial t} \tag{2}$$

$$\nabla \times \vec{E} = -\mu \frac{\partial \vec{H}}{\partial t} \tag{3}$$

where, ε and μ represent the permittivity and permeability, respectively.

In the HIE technique [29, 30], E_x and H_x fields are defined at time steps $n - 1/2$ and $n + 1/2$, and other fields components are defined at time steps n and $n + 1$. For E_x and H_x components, we use the explicit-difference technique at integer time step n , whereas for other components, we use semi-implicit difference technique at time step $n + 1/2$. By applying the HIE technique [29, 30] to (2) and (3), Maxwell’s equations can be written in a matrix form as,

$$\partial_t E = \frac{A}{\varepsilon} H \tag{4}$$

$$\partial_t H = -\frac{A}{\mu} E \tag{5}$$

where $E = [E_x^n, E_y^{n+1/2}, E_z^{n+1/2}]^T$, $H = [H_x^n, H_y^{n+1/2}, H_z^{n+1/2}]^T$ and

$$A = \begin{bmatrix} 0 & -\partial_z & \partial_y \\ \partial_z & 0 & -\partial_x/2 \\ -\partial_y & \partial_x/2 & 0 \end{bmatrix} \tag{6}$$

$\partial_t, \partial_x, \partial_y, \partial_z$ are the first-order central difference operators for time and space axes, respectively. By discretizing (4) and (5), we can obtain the difference updating equations as

$$\begin{aligned} E_x^{n+1/2} \Big|_{i+1/2,j,k} &= E_x^{n-1/2} \Big|_{i+1/2,j,k} \\ &+ \frac{\Delta t}{\varepsilon \Delta y} \left(H_z^n \Big|_{i+1/2,j+1/2,k} - H_z^n \Big|_{i+1/2,j-1/2,k} \right) \\ &- \frac{\Delta t}{\varepsilon \Delta z} \left(H_y^n \Big|_{i+1/2,j,k+1/2} - H_y^n \Big|_{i+1/2,j,k-1/2} \right) \end{aligned} \quad (7)$$

$$\begin{aligned} E_y^{n+1} \Big|_{i,j+1/2,k} &= \frac{\Delta t}{\varepsilon \Delta z} \left(H_x^{n+1/2} \Big|_{i,j+1/2,k+1/2} - H_x^{n+1/2} \Big|_{i,j+1/2,k-1/2} \right) \\ &+ E_y^n \Big|_{i,j+1/2,k} - \frac{\Delta t}{2\varepsilon \Delta x} \left(H_z^{n+1} \Big|_{i+1/2,j+1/2,k} - H_z^{n+1} \Big|_{i-1/2,j+1/2,k} \right. \\ &\left. + H_z^n \Big|_{i+1/2,j+1/2,k} - H_z^n \Big|_{i-1/2,j+1/2,k} \right) \end{aligned} \quad (8)$$

$$\begin{aligned} E_z^{n+1} \Big|_{i,j,k+1/2} &= E_z^n \Big|_{i,j,k+1/2} \\ &- \frac{\Delta t}{\varepsilon \Delta y} \left(H_x^{n+1/2} \Big|_{i,j+1/2,k+1/2} - H_x^{n+1/2} \Big|_{i,j-1/2,k+1/2} \right) \\ &+ \frac{\Delta t}{2\varepsilon \Delta x} \left(H_y^{n+1} \Big|_{i+1/2,j,k+1/2} - H_y^{n+1} \Big|_{i-1/2,j,k+1/2} \right. \\ &\left. + H_y^n \Big|_{i+1/2,j,k+1/2} - H_y^n \Big|_{i-1/2,j,k+1/2} \right) \end{aligned} \quad (9)$$

$$\begin{aligned} H_x^{n+1/2} \Big|_{i,j+1/2,k+1/2} &= H_x^{n-1/2} \Big|_{i,j+1/2,k+1/2} \\ &+ \frac{\Delta t}{\mu \Delta z} \left(E_y^n \Big|_{i,j+1/2,k+1} - E_y^n \Big|_{i,j+1/2,k} \right) \\ &- \frac{\Delta t}{\mu \Delta y} \left(E_z^n \Big|_{i,j+1,k+1/2} - E_z^n \Big|_{i,j,k+1/2} \right) \end{aligned} \quad (10)$$

$$\begin{aligned} H_y^{n+1} \Big|_{i+1/2,j,k+1/2} &= H_y^n \Big|_{i+1/2,j,k+1/2} \\ &- \frac{\Delta t}{\mu \Delta z} \left(E_x^{n+1/2} \Big|_{i+1/2,j,k+1} - E_x^{n+1/2} \Big|_{i+1/2,j,k} \right) \\ &+ \frac{\Delta t}{2\mu \Delta x} \left(E_z^{n+1} \Big|_{i+1,j,k+1/2} - E_z^{n+1} \Big|_{i,j,k+1/2} \right. \\ &\left. + E_z^n \Big|_{i+1,j,k+1/2} - E_z^n \Big|_{i,j,k+1/2} \right) \end{aligned} \quad (11)$$

$$\begin{aligned} H_z^{n+1} \Big|_{i+1/2,j+1/2,k} &= H_z^n \Big|_{i+1/2,j+1/2,k} \\ &+ \frac{\Delta t}{\mu \Delta y} \left(E_x^{n+1/2} \Big|_{i+1/2,j+1,k} - E_x^{n+1/2} \Big|_{i+1/2,j,k} \right) \end{aligned}$$

$$\begin{aligned}
 & -\frac{\Delta t}{2\mu\Delta x} \left(E_y^{n+1} \Big|_{i+1,j+1/2,k} - E_y^{n+1} \Big|_{i,j+1/2,k} \right. \\
 & \left. + E_y^n \Big|_{i+1,j+1/2,k} - E_y^n \Big|_{i,j+1/2,k} \right) \tag{12}
 \end{aligned}$$

n and Δt are the index and size of the time step; Δx , Δy , Δz are the space increments in x - y - and z -directions, respectively; i , j , k are the indices of space increments in x - y - and z -directions, respectively.

Using the TF/SF technique [16], by combining with the CTW wave we can obtain the difference updating equations for the HIE-SFDTD method as,

$$\begin{aligned}
 E_x^{n+1/2} \Big|_{i+1/2,j,k} &= E_x^{n-1/2} \Big|_{i+1/2,j,k} \\
 &+ \frac{\Delta t}{\varepsilon\Delta y} \left(H_z^n \Big|_{i+1/2,j+1/2,k} - H_z^n \Big|_{i+1/2,j-1/2,k} \right) \\
 &- \frac{\Delta t}{\varepsilon\Delta z} \left(\left(H_y^n \Big|_{i+1/2,j,k+1/2} + \delta H_y^n \Big|_{i+1/2,j,k+1/2}^{\text{CTW}} \right) - H_y^n \Big|_{i+1/2,j,k-1/2} \right) \tag{13}
 \end{aligned}$$

$$\begin{aligned}
 E_y^{n+1} \Big|_{i,j+1/2,k} &= \frac{\Delta t}{\varepsilon\Delta z} \left(\left(H_x^{n+1/2} \Big|_{i,j+1/2,k+1/2} + \delta H_x^{n+1/2} \Big|_{i,j+1/2,k+1/2}^{\text{CTW}} \right) \right. \\
 &\left. - H_x^{n+1/2} \Big|_{i,j+1/2,k-1/2} \right) + E_y^n \Big|_{i,j+1/2,k} \\
 &- \frac{\Delta t}{2\varepsilon\Delta x} \left(H_z^{n+1} \Big|_{i+1/2,j+1/2,k} - H_z^{n+1} \Big|_{i-1/2,j+1/2,k} \right) \\
 &+ H_z^n \Big|_{i+1/2,j+1/2,k} - H_z^n \Big|_{i-1/2,j+1/2,k} \tag{14}
 \end{aligned}$$

$$\begin{aligned}
 E_z^{n+1} \Big|_{i,j,k+1/2} &= E_z^n \Big|_{i,j,k+1/2} \\
 &- \frac{\Delta t}{\varepsilon\Delta y} \left(H_x^{n+1/2} \Big|_{i,j+1/2,k+1/2} - H_x^{n+1/2} \Big|_{i,j-1/2,k+1/2} \right) \\
 &+ \frac{\Delta t}{2\varepsilon\Delta x} \left(H_y^{n+1} \Big|_{i+1/2,j,k+1/2} - H_y^{n+1} \Big|_{i-1/2,j,k+1/2} \right) \\
 &+ H_y^n \Big|_{i+1/2,j,k+1/2} - H_y^n \Big|_{i-1/2,j,k+1/2} \tag{15}
 \end{aligned}$$

$$\begin{aligned}
 H_x^{n+1/2} \Big|_{i,j+1/2,k+1/2} &= H_x^{n-1/2} \Big|_{i,j+1/2,k+1/2} \\
 &+ \frac{\Delta t}{\mu\Delta z} \left(E_y^n \Big|_{i,j+1/2,k+1} - \left(E_y^n \Big|_{i,j+1/2,k} + \delta E_y^n \Big|_{i,j+1/2,k}^{\text{CTW}} \right) \right) \\
 &- \frac{\Delta t}{\mu\Delta y} \left(E_z^n \Big|_{i,j+1,k+1/2} - E_z^n \Big|_{i,j,k+1/2} \right) \tag{16}
 \end{aligned}$$

$$\begin{aligned}
 H_y^{n+1} \Big|_{i+1/2,j,k+1/2} &= H_y^n \Big|_{i+1/2,j,k+1/2} \\
 &- \frac{\Delta t}{\mu\Delta z} \left(E_x^{n+1/2} \Big|_{i+1/2,j,k+1} - \left(E_x^{n+1/2} \Big|_{i+1/2,j,k} + \delta E_x^{n+1/2} \Big|_{i+1/2,j,k}^{\text{CTW}} \right) \right)
 \end{aligned}$$

$$\begin{aligned}
& + \frac{\Delta t}{2\mu\Delta x} \left(E_z^{n+1} \Big|_{i+1,j,k+1/2} - E_z^{n+1} \Big|_{i,j,k+1/2} \right. \\
& \left. + E_z^n \Big|_{i+1,j,k+1/2} - E_z^n \Big|_{i,j,k+1/2} \right) \tag{17}
\end{aligned}$$

$$\begin{aligned}
& H_z^{n+1} \Big|_{i+1/2,j+1/2,k} = H_z^n \Big|_{i+1/2,j+1/2,k} \\
& + \frac{\Delta t}{\mu\Delta y} \left(E_x^{n+1/2} \Big|_{i+1/2,j+1,k} - E_x^{n+1/2} \Big|_{i+1/2,j,k} \right) \\
& - \frac{\Delta t}{2\mu\Delta x} \left(E_y^{n+1} \Big|_{i+1,j+1/2,k} - E_y^{n+1} \Big|_{i,j+1/2,k} \right. \\
& \left. + E_y^n \Big|_{i+1,j+1/2,k} - E_y^n \Big|_{i,j+1/2,k} \right) \tag{18}
\end{aligned}$$

where $\delta = 1$ at the TF/SF surface, else $\delta = 0$.

It can be seen from these equations that (13) and (16) for $E_x^{n+1/2}$ and $H_x^{n+1/2}$ can be updated directly by using the foregone field components. However, Eqs. (14), (15), (17) and (18) cannot be solved directly, because they all contain unknown components on both sides of the equations. Thus, the unknown components on the right-hand sides need to be eliminated. Updating of the E_y^{n+1} component in (14) needs the unknown H_z^{n+1} components, substituting (18) into (14) and by appropriate rearrangement, we obtain the equation for E_y^{n+1}

$$\begin{aligned}
& aE_y^{n+1} \Big|_{i-1,j+1/2,k} + bE_y^{n+1} \Big|_{i,j+1/2,k} + aE_y^{n+1} \Big|_{i+1,j+1/2,k} \\
& = \frac{\varepsilon}{\Delta t} E_y^n \Big|_{i,j+1/2,k} + \delta/\Delta z \times H_x^{n+1/2} \Big|_{i,j+1/2,k+1/2}^{\text{CTW}} \\
& \left(-\frac{1}{\Delta x} \left(H_z^n \Big|_{i+1/2,j+1/2,k} - H_z^n \Big|_{i-1/2,j+1/2,k} \right) \right. \\
& \left. + \frac{1}{\Delta z} \left(H_x^{n+1/2} \Big|_{i,j+1/2,k+1/2} - H_x^{n+1/2} \Big|_{i,j+1/2,k-1/2} \right) \right) \\
& - \frac{\Delta t}{2\mu\Delta x\Delta y} \left(E_x^{n+1/2} \Big|_{i+1/2,j+1,k} - E_x^{n+1/2} \Big|_{i+1/2,j,k} \right) \\
& - a \left(E_y^n \Big|_{i+1,j+1/2,k} - 2E_y^n \Big|_{i,j+1/2,k} + E_y^n \Big|_{i-1,j+1/2,k} \right) \tag{19}
\end{aligned}$$

where $a = -\Delta t/(4\mu\Delta x^2)$, $b = (\varepsilon/\Delta t + \Delta t/(2\mu\Delta x^2))$. Similarly, updating the E_z^{n+1} component needs the unknown H_y^{n+1} components. Substituting (17) into (15), we have

$$\begin{aligned}
& aE_z^{n+1} \Big|_{i-1,j,k+1/2} + bE_z^{n+1} \Big|_{i,j,k+1/2} + aE_z^{n+1} \Big|_{i+1,j,k+1/2} \\
& = \frac{1}{\Delta x} \left(H_y^n \Big|_{i+1/2,j,k+1/2} - H_y^n \Big|_{i-1/2,j,k+1/2} \right)
\end{aligned}$$

$$\begin{aligned}
 & -\frac{1}{\Delta y} \left(H_x^{n+1/2} \Big|_{i,j+1/2,k+1/2} - H_x^{n+1/2} \Big|_{i,j-1/2,k+1/2} \right) \\
 & -a \left(E_z^n \Big|_{i+1,j,k+1/2} - 2E_z^n \Big|_{i,j,k+1/2} + E_z^n \Big|_{i-1,j,k+1/2} \right) - \frac{\Delta t}{2\mu\Delta x\Delta z} \\
 & \left(\begin{aligned}
 & E_x^{n+1/2} \Big|_{i+1/2,j,k+1} - E_x^{n+1/2} \Big|_{i+1/2,j,k} + \delta E_x^{n+1/2} \Big|_{i+1/2,j,k}^{\text{CTW}} \\
 & -E_x^{n+1/2} \Big|_{i-1/2,j,k+1} + E_x^{n+1/2} \Big|_{i-1/2,j,k} - \delta E_x^{n+1/2} \Big|_{i-1/2,j,k}^{\text{CTW}}
 \end{aligned} \right) \\
 & + \frac{\varepsilon}{\Delta t} E_z^n \Big|_{i,j,k+1/2} \tag{20}
 \end{aligned}$$

From the equations above, we find on the right-hand side of the equation that the terms are previous field components, so (19) and (20) can be solved implicitly. After E_y^{n+1} and E_z^{n+1} are obtained, H_z^{n+1} and H_y^{n+1} are explicitly updated by using (17) and (18).

3.2. Handling of the Periodic Boundary Condition

In our work, the incident wave is considered as a constant transverse wave-number wave, presented in Eq. (1). For k_x , k_y are independent of frequency, there are no time delay in the x - y plane, so the PBC for the CTW wave can be implemented in the same way as the PBC for normal incident [16, 27]

$$E_y^{n+1} \left(N_{x1} - 1, j + \frac{1}{2}, k \right) = E_y^{n+1} \left(N_{x4} - 1, j + \frac{1}{2}, k \right) e^{-\tilde{j}k_x P_x} \tag{21}$$

$$E_y^{n+1} \left(N_{x4}, j + \frac{1}{2}, k \right) = E_y^{n+1} \left(N_{x1}, j + \frac{1}{2}, k \right) e^{\tilde{j}k_x P_x} \tag{22}$$

$$E_z^{n+1} \left(N_{x1} - 1, j, k + \frac{1}{2} \right) = E_z^{n+1} \left(N_{x4} - 1, j, k + \frac{1}{2} \right) e^{-\tilde{j}k_x P_x} \tag{23}$$

$$E_z^{n+1} \left(N_{x4}, j, k + \frac{1}{2} \right) = E_z^{n+1} \left(N_{x1}, j, k + \frac{1}{2} \right) e^{\tilde{j}k_x P_x} \tag{24}$$

where, N_{x1} , N_{x4} represent the nodes of electric field on the unit cell boundary. $P_x = N_{x4}\Delta x$ is the dimension of the unit cell in the x -direction.

By substituting (21)–(24) into (19), we can get

$$[\mathbf{M}] \vec{E}_y = \vec{\xi} \tag{25}$$

where $\vec{\xi}$ represents the right-hand vector of (19) and \vec{E}_y is unknown in general. $[\mathbf{M}]$ is obtained from (19) for each column of E_y , so (19)

can be written as

$$\begin{bmatrix} b & a & & & \alpha \\ a & b & a & & \\ & \dots & \dots & \dots & \\ & & a & b & a \\ \beta & & & a & b \end{bmatrix} \begin{bmatrix} E_y^{n+1} |_{N_{x1}, j+1/2, k} \\ E_y^{n+1} |_{N_{x1+1}, j+1/2, k} \\ E_y^{n+1} |_{N_{x1+2}, j+1/2, k} \\ \vdots \\ E_y^{n+1} |_{N_{x4-1}, j+1/2, k} \end{bmatrix} = \begin{bmatrix} \xi(N_{x1}) \\ \xi(N_{x1+1}) \\ \xi(N_{x1+2}) \\ \vdots \\ \xi(N_{x4-1}) \end{bmatrix} \quad (26)$$

where $\alpha = a \cdot e^{-\tilde{j}k_x P_x}$, $\beta = a \cdot e^{\tilde{j}k_x P_x}$.

The coefficient matrix $[\mathbf{M}]$ is not a tridiagonal matrix, so it cannot be solved with the efficient forward-elimination and backward-substitution method directly. By using the Sherman Morrison formula [31], two auxiliary linear problems are defined [31].

$$[\mathbf{N}] \vec{E}_{y1} = \vec{\xi} \quad (27)$$

$$[\mathbf{N}] \vec{E}_{y2} = \vec{v}_1 \quad (28)$$

$$[\mathbf{N}] = [\mathbf{M}] - \vec{v}_1 \vec{v}_2^T \quad (29)$$

$$\vec{v}_1 = \vec{v}_2 = [\alpha^{1/2} \quad 0 \quad \dots \quad 0 \quad \beta^{1/2}]^T \quad (30)$$

So the solution of (26) is obtained via

$$\vec{E}_y = \vec{E}_{y1} + \varsigma \vec{E}_{y2} \quad (31)$$

$$\varsigma = -\frac{\vec{v}_2^T \vec{E}_{y1}}{1 + \vec{v}_2^T \vec{E}_{y2}} \quad (32)$$

By observation, one can find that matrix $[\mathbf{M}]$ in (26) is related to matrix $[\mathbf{N}]$.

$$[\mathbf{N}] = \begin{bmatrix} b & a & 0 & \dots & 0 \\ a & b & a & \dots & 0 \\ 0 & \ddots & \ddots & \dots & \vdots \\ \vdots & \dots & a & b & a \\ 0 & \dots & 0 & a & b \end{bmatrix} \quad (33)$$

Because $[\mathbf{N}]$ is a tridiagonal matrix, the auxiliary linear problems can be solved efficiently by using forward-elimination and backward-substitution method [32]. Eq. (20) can be solved in the same way.

From the equations derived above, it can be seen that at each time step, the proposed method requires solution of two un-tridiagonal matrices when the PBC is applied to and four explicit updates, while it needs to solve six matrices and six explicit updates in ADI-SFDTD scheme. Therefore, we can conclude the proposed HIE-SFDTD method is simpler than ADI-SFDTD method.

3.3. Numerical Stability

To satisfy the stability condition, the limitation for the time step size for SFDTD can be calculated as follows [16],

$$\Delta t \leq \frac{1}{c\sqrt{\Delta x^{-2} + \Delta y^{-2} + \Delta z^{-2}}} \quad (34)$$

However, for the HIE-SFDTD method the maximum time increment [30] is

$$\Delta t \leq \frac{1}{c\sqrt{\Delta y^{-2} + \Delta z^{-2}}} \quad (35)$$

which is independent of Δx . This is especially useful when the simulated structure has a fine-scale dimension in one direction. A small spatial increment can be used in the direction with fine scale and a larger spatial increment can be used in the direction with coarse scale. If we perform the implicit-difference scheme in the direction with a larger spatial increment, the time step size is thus determined by the larger spatial increments. For example, the sizes of the structure in the directions y and z are larger than that in the x direction. By setting $\Delta y = \Delta z = 5\Delta x$, the maximum time step size meeting the stability condition of the HIE-SFDTD algorithm can be determined by Eq. (35), that is $\Delta t = \frac{\Delta y}{c\sqrt{2}}$, while the maximum time step size for the conventional SFDTD method is $\Delta t = \frac{1}{c\sqrt{\Delta x^{-2} + \Delta y^{-2} + \Delta z^{-2}}} = \frac{\Delta y}{c\sqrt{27}}$. As a result, computational resources can be saved considerably.

4. SIMULATION RESULTS

To demonstrate the proposed HIE-SFDTD method, two examples are presented. Simulations are carried out using the HIE-SFDTD method, conventional SFDTD method, and ADI-SFDTD method for comparison.

In the first example, the HIE-SFDTD method is applied to calculate the reflection coefficient phase for the grounded slab, shown in Fig. 4. The structure is composed of a 5 mm thick dielectric slab backed by a PEC plate. This structure is chosen because of the availability of analytical results. The periodic unit cell is chosen 5 mm \times 5 mm in x and y directions. The space increments are chosen $\Delta y = \Delta z = 5\Delta x = 1$ mm, the time increment is $\Delta t = 0.866e - 12$ s. The σ is chosen 314 m^{-1} corresponds to $f = 15$ GHz bandwidth for Gaussian pulse. The transverse wave-numbers are chosen $k_y = 0$, k_x ranges from 5π to $90\pi \text{ mm}^{-1}$.

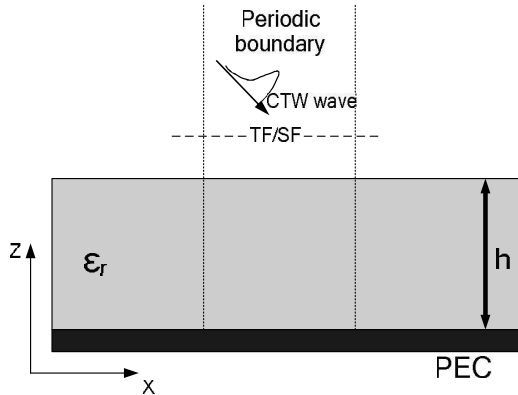


Figure 4. The grounded slab with $h = 5$ mm, $\epsilon_r = 4.0$.

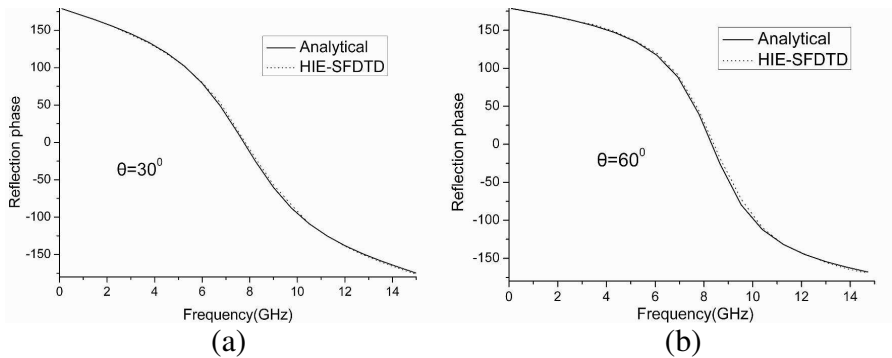


Figure 5. Comparison of HIE-SFDTD results with the analytical results for (a) $\theta = 30^\circ$ and (b) $\theta = 60^\circ$.

The reflection coefficient phases are calculated for $\theta = 30^\circ, 60^\circ$, shown in Fig. 5. The calculated results are compared with the analytical results. We can see that they agree well with each other. This verifies the validity of the HIE-SFDTD method.

In the second example, a periodic array of metallic patches with thin slots along x axis plotted in Fig. 6 is presented. $T_x = T_y = 10$ mm, $W = L = 5$ mm. The sizes of the slots are 0.1 mm. The space increments are chosen as $\Delta y = \Delta z = 5\Delta x = \Delta = 0.5$ mm. And the computational domain is truncated by 8-layer PML in the z direction. So it contains $100 \times 20 \times 86$ cells. The CTW wave is introduced into the computational domain, with the transverse wave-number k_x ranges from 20 m^{-1} to 800 m^{-1} . As the CFL condition is weaker than the conventional FDTD method, the time step size in the HIE-FDTD can be larger than the conventional FDTD method, so to

run the same simulation, CPU time can be saved. In the example, we first choose the same time-steps for conventional SFDTD, HIE-SFDTD and ADI-SFDTD, results are shown in Fig. 7. To show the advantage of the proposed HIE-SFDTD, we also choose different time-steps. For conventional SFDTD 2.78×10^{-13} s is chosen, and for the proposed method and the ADI-SFDTD method 11.12×10^{-13} s is chosen. Simulation results are shown in Fig. 8.

Figure 7 shows the reflection coefficient of the periodic array of metallic patches with the time step 2.78×10^{-13} s for the conventional SFDTD, HIE-SFDTD and ADI-SFDTD methods, respectively. It can be seen from these figures that the proposed HIE-SFDTD method and ADI-SFDTD method agree well with the conventional SFDTD method. From Fig. 8 we can see that when the time step increases, the HIE-SFDTD results still achieve good agreement with the conventional SFDTD results, while ADI-SFDTD results have a deviation from the conventional results, especially in the high frequencies. It is apparent

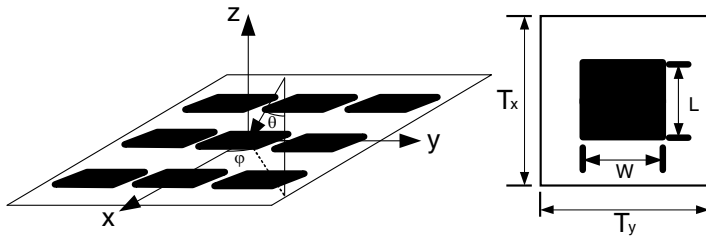


Figure 6. Periodic array of metallic patches with thin slots.

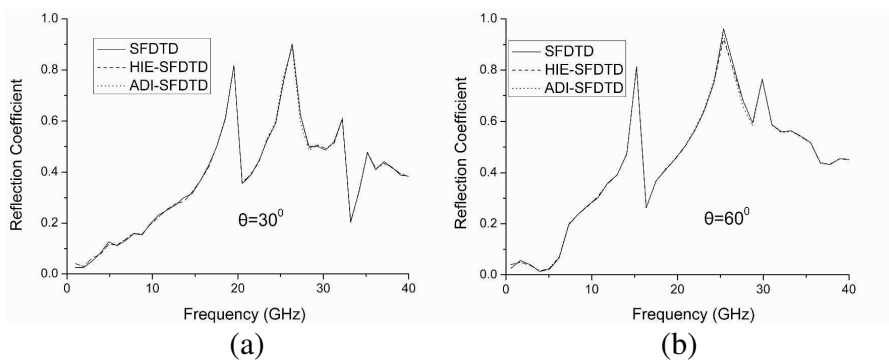


Figure 7. Reflection coefficients for the conventional SFDTD ($\Delta t = 2.78 \times 10^{-13}$ s), the HIE-SFDTD ($\Delta t = 2.78 \times 10^{-13}$ s) and the ADI-SFDTD ($\Delta t = 2.78 \times 10^{-13}$ s) method for $\theta = 30^\circ$ and $\theta = 60^\circ$.

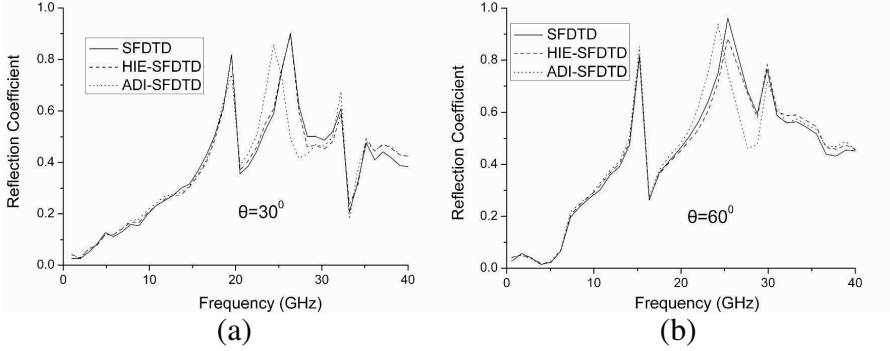


Figure 8. Reflection coefficients for the conventional SFTD ($\Delta t = 2.78 \times 10^{-13}$ s), the HIE-SFTD ($\Delta t = 11.12 \times 10^{-13}$ s) and the ADI-SFTD ($\Delta t = 11.12 \times 10^{-13}$ s) method for $\theta = 30^\circ$ and $\theta = 60^\circ$.

that the proposed method has higher accuracy than the ADI-SFTD method.

Finally, we mention the computational efficiency of the proposed HIE-SFTD method. On a Core2 2.4-GHz machine, it took the conventional SFTD method 17354 seconds and the HIE-SFTD method (with time step size 11.12×10^{-13} s) 8406 seconds to run the same simulation, which is 18477 seconds in the ADI-SFTD method. So compared with the ADI-SFTD method, the proposed method has higher efficiency. The CPU running time for this method can be reduced to about 45% of the ADI-SFTD method.

5. CONCLUSION

In this paper, we present a hybrid implicit-explicit SFTD method to solve periodic structures at oblique incidence. Numerical results indicate that the proposed method is accurate and efficient. The CPU time for the proposed method can be reduced to about 45% of the ADI-SFTD method. For the same time step size, the proposed method has higher efficiency than ADI-SFTD method and also higher accuracy. To extend this method to solve anisotropic medium is our future work [33–35].

ACKNOWLEDGMENT

This work was supported by the National Natural Science Foundation of China under Grant No. 60971063.

REFERENCES

1. Wang, X., M. Zhang, and S.-J. Wang, "Practicability analysis and application of PBG structures on cylindrical conformal microstrip antenna and array," *Progress In Electromagnetics Research*, Vol. 115, 495–507, 2011.
2. Yang, P., F. Yang, and Z.-P. Nie, "DOA estimation with sub-array divided technique and interpolated esprit algorithm on a cylindrical conformal array antenna," *Progress In Electromagnetics Research*, Vol. 103, 201–216, 2010.
3. Li, R., L. Xu, X. W. Shi, L. Chen, and C. Y. Cui, "Two-dimensional NC-music DOA estimation algorithm with a conformal cylindrical antenna array," *Journal of Electromagnetic Waves and Applications*, Vol. 25, Nos. 5–6, 805–818, 2011.
4. Kshetrimayum, R. S. and L. Zhu, "Guided-wave characteristics of waveguide based periodic structures loaded with various FSS strip layers," *IEEE Transactions on Antennas and Propagation*, Vol. 53, 120–124, 2005.
5. Dardenne, X. and C. Craeye, "Method of Moments simulation of infinitely periodic structures combining metal with connected dielectric objects," *IEEE Transactions on Antennas and Propagation*, Vol. 56, 2372–2380, 2008.
6. Petersson, L. E. R. and J.-M. Jin, "A two-dimensional time-domain finite element formulation for periodic structures," *IEEE Transactions on Antennas and Propagation*, Vol. 53, 1480–1488, 2005.
7. Yee, K. S., "Numerical solution of initial boundary value problems involving Maxwell's equations in isotropic media," *IEEE Transactions on Antennas and Propagation*, Vol. 14, 302–307, 1966.
8. Xiong, R., B. Chen, Y.-F. Mao, and Y. Yi, "The capacitance thin-slot formalism revisited: An alternative expression for the thin-slot penetration," *Journal of Electromagnetic Waves and Applications*, Vol. 26, No. 4, 446–458, 2012.
9. Cai, Z.-Y., B. Chen, Q. Yin, and R. Xiong, "The WLP-FDTD method for periodic structures with oblique incident wave," *IEEE Transactions on Antennas and Propagation*, Vol. 59, 3780–3785, 2011.
10. Lee, K. H., I. Ahmed, R. S. M. Goh, E. H. Khoo, E. P. Li, and T. G. G. Hung, "Implementation of the FDTD method based on Lorentz-Drude dispersive model on GPU for plasmonics applications," *Progress In Electromagnetics Research*, Vol. 116,

- 441–456, 2011.
11. Izadi, M., M. Z. A. Ab Kadir, C. Gomes, and W. F. W. Ahmad, “An analytical second-FDTD method for evaluation of electric and magnetic fields at intermediate distances from lightning channel,” *Progress In Electromagnetics Research*, Vol. 110, 329–352, 2010.
 12. Chen, H.-L., B. Chen, Y. Yi, and D.-G. Fang, “Unconditionally stable ADI-BOR-FDTD algorithm for the analysis of rotationally symmetric geometries,” *IEEE Microw. Wireless Compon. Lett.*, Vol. 17, 304–306, 2007.
 13. Yi, Y., B. Chen, W.-X. Sheng, and Y.-L. Pei, “A memory-efficient formulation of the unconditionally stable FDTD method for solving Maxwell’s equations,” *IEEE Transactions on Antennas and Propagation*, Vol. 55, 3729–3722, 2007.
 14. Duan, Y.-T., B. Chen, and Y. Yi, “Efficient implementation for the unconditionally stable 2-D WLP-FDTD method,” *IEEE Microw. Wireless Compon. Lett.*, Vol. 19, 677–679, 2009.
 15. Xiao, S.-Q., Z. H. Shao, and B.-Z. Wang, “Application of the improved matrix type FDTD method for active antenna analysis,” *Progress In Electromagnetics Research*, Vol. 100, 245–263, 2010.
 16. Taflove, A. and S. C. Hagness, *Computational Electrodynamics: The Finite-Difference Time-Domain Method*, 2nd Edition, Artech House, Boston, MA, 2000.
 17. Wang, S., J. Chen, and P. Ruchhoeft, “An ADI-FDTD method for periodic structures,” *IEEE Transactions on Antennas and Propagation*, Vol. 53, 2343–2346, 2005.
 18. Singh, G., E.-L. Tan, and Z.-N. Chen, “Efficient complex envelope ADI-FDTD method for the analysis of anisotropic photonic crystals,” *IEEE Photonics Technology Letters*, Vol. 23, 801–803, 2011.
 19. Mao Y.-F., B. Chen, H.-L. Chen, and Q. Wu, “Unconditionally stable SFDTD algorithm for solving oblique incident wave on periodic structures,” *IEEE Microw. Wireless Compon. Lett.*, Vol. 19, 257–259, 2009.
 20. Shibayama, J., R. Ando, J. Yamauchi, and H. Nakano, “An LOD-FDTD method for the analysis of periodic structures at normal incidence,” *IEEE Antennas and Wireless Propagation Letters*, Vol. 8, 890–893, 2009.
 21. Wakabayashi, Y., J. Shibayama, J. Yamauchi, and H. Nakano, “A locally one-dimensional finite difference time domain method for the analysis of a periodic structure at oblique incidence,” *Radio Science*, Vol. 46, 1–9, 2011.

22. Shibayama, J., R. Ando, J. Yamauchi, and H. Nakano, "Analysis of a photonic bandgap structure using a periodic LOD-FDTD method," *Microwave Conference, APMC*, 56–59, 2009.
23. Harms, P., R. Mittra, and K. Wai, "Implementation of the periodic boundary condition in the finite-difference time-domain algorithm for FSS structures," *IEEE Transactions on Antennas and Propagation*, Vol. 42, 1317–1324, 1994.
24. Amjadi, S. M. and M. Soleimani, "Design of band-pass waveguide filter using frequency selective surfaces loaded with surface mount capacitors based on split-field update FDTD method," *Progress In Electromagnetics Research B*, Vol. 3, 271–281, 2008.
25. Belkhir, A., O. Arar, S. S. Benabbes, O. Lamrous, and F. I. Baida, "Implementation of dispersion models in the split-field finite-difference-time-domain algorithm for the study of metallic periodic structures at oblique incidence," *Phys. Rev. E*, Vol. 81, 046705, 2010.
26. Shahmansouri, A. and B. Rashidian, "GPU implementation of split-field finite-difference time-domain method for Drude-Lorentz dispersive media," *Progress In Electromagnetics Research*, Vol. 125, 55–77, 2012.
27. Amir, A. and R.-S. Yahya, "Spectral FDTD: A novel technique for the analysis of oblique incident plane wave on periodic structures," *IEEE Transactions on Antennas and Propagation*, Vol. 54, 1818–1825, 2006.
28. Yang, F., A. Elsherbeni, and J. Chen, "A hybrid spectral-FDTD/ARMA method for periodic structure analysis," *IEEE Antennas and Propagation Society International Symposium*, 3720–3723, 2007.
29. Huang, B. K., G. Wang, and Y. S. Jiang, "A hybrid implicit-explicit FDTD scheme with weakly conditional stability," *Microwave and Optical Tech. Lett.*, Vol. 39, No. 2, 97–101, 2003.
30. Chen, J. and J. G. Wang, "A 3D hybrid implicit-explicit FDTD scheme with weakly conditional stability," *Microwave and Optical Tech. Lett.*, Vol. 48, No. 11, 2291–2294, 2006.
31. Thomas, J.-W., *Numerical Partial Differential Equations: Finite Difference Methods*, Springer Verlag, Berlin, Germany, 1995.
32. Zhao, A.-P., "Two special notes on the implementation of the unconditionally stable ADI-FDTD method," *Microwave and Optical Tech. Lett.*, Vol. 33, No. 4, 273–277, 2002.
33. Yu, Y. and J. J. Simpson, "An E-J Collocated 3-D FDTD model of electromagnetic wave propagation in magnetized cold plasma,"

- IEEE Transactions on Antennas and Propagation*, Vol. 58, No. 2, 469–478, February 2010.
34. Hu, W. and S. A. Cummer, “An FDTD model for low and high altitude lightning-generated EM fields,” *IEEE Transactions on Antennas and Propagation*, Vol. 54, 1513–1522, May 2006.
 35. Jung, K.-Y., F. L. Teixeira, and R. Lee, “Complex envelop PML-ADI-FDTD method for lossy anisotropic dielectrics,” *IEEE Antennas and Wireless Propagation Letters*, Vol. 6, 643–646, 2007.